Modeling the hydrological response to climate change in a glacierized high mountain region, northwest China

Meiping SUN,[1,2] Zhongqin LI,[2,1] Xiaojun YAO,[1,2] Mingjun ZHANG,[1] Shuang JIN[2]

[1]*College of Geography and Environmental Science, Northwest Normal University, Lanzhou, China*
[2]*State Key Laboratory of Cryospheric Sciences/Tianshan Glaciological Station, Cold and Arid Regions Environmental and Engineering Research Institute, Chinese Academy of Sciences, Lanzhou, China*
Correspondence: Meiping Sun <sunmeiping1982@163.com>

ABSTRACT. The impact of climate change on the variability of local discharge was investigated in a glacierized high mountain catchment located in the source area of the Ürümqi river, northwest China. We used past climate records to drive a hydrological model to simulate the discharge from 2000 to 2008. The model was then used to project future discharge variations for the period 2041–60, based on a regionally downscaled climate-change scenario combined with three stages of glacier coverage (i.e. compared to the glacier coverage in 2008): unchanged glacier size (100% glacierized), recession of half the glacier area (50% glacierized) and complete disappearance of glaciers (0% glacierized). In each scenario, snowmelt will begin half a month earlier and the discharge will increase in May. For the 100% glacierized scenario, the discharge will increase by 66 ± 35% in a smaller (3.34 km^2) and more glaciated (50%) catchment and 33 ± 20% in a larger (28.90 km^2) and proportionally less glaciated (18%) catchment. If the glacier area reduces by half, the discharge will decrease by 8 ± 5% and 9 ± 6%, respectively. Once the glacier disappears, the discharge will decrease by 58 ± 20% and 40 ± 13%, respectively. Together, the results indicate that a warming climate and the resulting glacier shrinkage will cause significant changes in the volume and timing of runoff.

KEYWORDS: climate change, glacier hydrology, mountain glaciers

INTRODUCTION

Glaciated high mountainous areas are source regions for many important rivers around the world. These 'water towers' supply water to the surrounding lowlands and have even greater significance in arid regions, especially under the influence of climate warming (Viviroli and others, 2007; Immerzeel and others, 2010). As in many mountain regions worldwide, the majority of mountain glaciers in China are currently in a state of rapid retreat and thinning (Liu and others, 1999, 2006; Shangguan and others, 2007). Over the past three decades, a strong pattern of deglaciation has occurred in the arid region of northwest China, with a 10–13.8% reduction in glacier area (Liu and others, 2003; Li and others, 2010a). The primary impact of these changes is exhibited through changes in discharge of glacier-fed rivers (Mark and Seltzer, 2003; Hagg and others, 2007). This is important because glacier melt helps to maintain streamflow during dry periods, whereas in non-glaciated basins, rivers would experience extremely low flow (Stahl and others, 2008).

According to the Intergovernmental Panel on Climate Change (IPCC), the predicted changes in temperature and precipitation are expected to cause mountain glaciers to retreat further during the 21st century, and in turn to substantially affect glacier melt and water availability (Solomon and others, 2007). We selected the Ürümqi river source region, a glaciated high mountain catchment in northwest China, as our study area. In this region, glaciers are relatively small, with an average area of <1 km^2, and are extremely sensitive to climate change. Li and others (2011) reported that from 1962 to 2008 the regional temperature increased by 1°C and the mass loss from Ürümqi glacier No. 1 (area 1.65 km^2 and length 2.23 km in 2009) was as much as 13.69 m. Given the relatively high sensitivity of smaller glaciers and the source area of the Ürümqi river as a major experimental base of cold region hydrology in China, with excellent glaciological, hydrological and meteorological monitoring records, our study site is highly useful for quantifying the magnitude and for clarifying the mechanisms of hydrological response processes in small glaciers under future climate conditions.

On a catchment scale, previous studies of the Ürümqi river source area have addressed the importance of glaciers and snowmelt and the potential effects of climate change on local hydrological regimes (Ye and others, 2005; Han and others, 2010; Li and others, 2010b; Sun and others, 2013). However, these results are mostly qualitative, and have not quantitatively evaluated the possible future changes in discharge. The objective of this research was to investigate how the water availability from this glaciated headwater might change by mid-century (2041–60) for three different scenarios of glacier coverage. First, we used the observed climate record to drive a hydrological model that simulated the discharge for the reference period 2000–08. The model was then used to predict future discharge variations, based on regionally downscaled climate change data. Such analyses are useful for evaluating the utilization of water resources and the development of appropriate watershed management strategies in the arid region of northwest China.

STUDY AREA

The Ürümqi river source region (43°05′–43°09′ N, 86°47′–86°53′ E; 3405–4486 m a.s.l.) is located on the northern side of the eastern Tien Shan, within the arid region of northwest China (Fig. 1). There are seven glaciers, with an area of

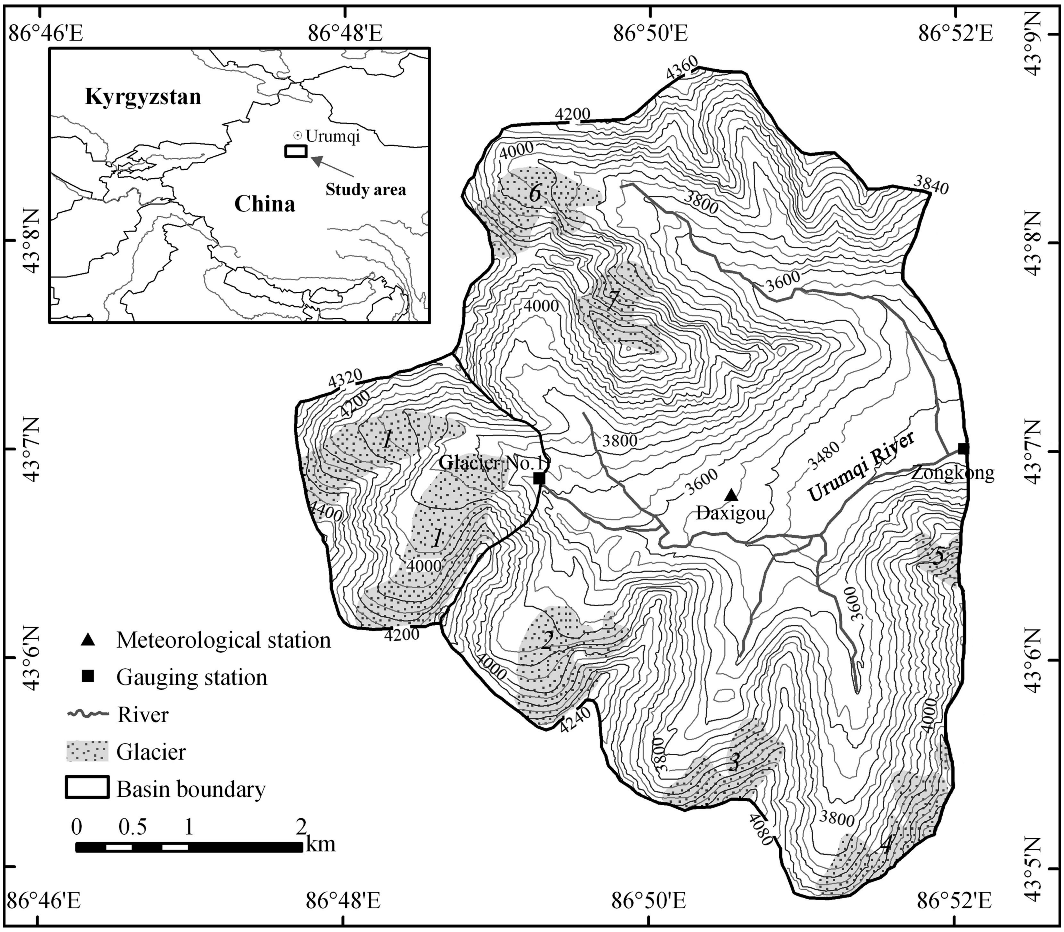

Fig. 1. Map of the Ürümqi river source region showing the locations of glaciers and hydrological and meteorological stations.

5.20 km^2, in this region. The catchment provides the principal water supply to the Ürümqi river, which is used for agricultural irrigation, and domestic water supplies in the city of Ürümqi. A westerly circulation prevails across the catchment throughout the year. According to Daxigou meteorological station, located within the investigation area, annual precipitation is ~490 mm, 88% of which falls between May and September, and the mean annual temperature is ~–5.1°C. Approximately 80% of the area is covered by bare soil, rock and alpine meadow. The soils are mainly alpine meadow varieties, which are little developed, with depths generally <20 cm (Shi and Kang, 1992). Only on the valley floor close to the river are the soils more developed and capable of storing small quantities of groundwater, so runoff is easily formed from rainfall and meltwater in the catchment.

Table 1. Principal geographical and hydrometeorological features of the two study-site sub-basins

	Ürümqi glacier No. 1	Zongkong
Drainage area (km^2)	3.34	28.90
Glaciation (%)	50	18
Elevation range (m a.s.l.)	3740–4486	3405–4486
Gauging station		
Latitude	43°06′ N	43°07′ N
Longitude	86°49′ E	86°52′ E
Elevation (m a.s.l.)	3693	3405
Annual total discharge (10^4 m^3)	241.81	1357.11
Observation period	1959–67,1979–2008	1985–2008
Mean annual temperature (°C)	–5.9	–4.9
Mean annual precipitation (mm)	504	463

There are two monitoring stations in the source region of the Ürümqi river. The glacier No. 1 monitoring station has operated below the terminus of glacier No. 1 since 1959. It covers a drainage area of 3.34 km^2, 50% of which is covered by glacier No. 1. The altitude of the catchment ranges from 3693 to 4486 m a.s.l. From 1962 to 2009, glacier No. 1 experienced an accelerated recession: its area diminished by 0.3 km^2 (15.6%) and its length by ~215 m (9.7%). The highly dynamic nature of the glacier has been particularly apparent since 1993, when it separated into two small independent branches due to enhanced melting. The Zongkong monitoring station, which commenced operations in 1985, is situated at the basin outlet. Its drainage area is 28.90 km^2. There are seven glaciers, including glacier No. 1, located in the Zongkong catchment, with 18% of the area glaciated, providing a larger and proportionally less glaciated catchment than glacier No. 1 catchment. Its altitude ranges from 3405 to 4486 m a.s.l. Table 1 lists the principal geographical and hydrometeorological characteristics of the two sub-basins.

DATASETS AND METHODS

Two key datasets that our study uses consist of discharge records from the glacier No. 1 and Zongkong monitoring stations (Fig. 1). It should be noted that the lengths of the observed records of the two monitoring stations differ and that some data were missing in 1996, when a great flood destroyed the two hydrologic sections. We used the discharge records from 1985 to 2008 (excluding 1996) to calibrate and validate the HBV (Hydrologiska Byrans Vattenbalansavdelning) hydrological model, which we used to examine the impact of climate change on future water resources. We also used long-term meteorological records (in particular, daily observed temperature and precipitation) from Daxigou meteorological station, located at 3539 m a.s.l., ~3 km downstream of glacier No. 1. For future climate data, we used the projected monthly temperature and precipitation data from the RegCM3 regional climate model. These data were spatially distributed using a digital elevation model (DEM) derived from a 1 : 50 000 topographic map. The measured mass balance of glacier No. 1 was also used to determine the hydrological parameters in a glacial runoff simulation. Finally, our study uses a 1 : 100 000 map of land use (Liu and others, 2014) to distinguish different storage and flow processes. The climate model and the hydrological model are described in more detail below.

RegCM3 regional climate model

We used the ICTP RegCM3 regional climate model, which was based on the model proposed by Giorgi and others (1993a,b) and refined by Pal and others (2007). The RegCM3 model employed the IPCC SRES (Special Report on Emissions Scenarios) A1B greenhouse gas emission scenario, a mid-range scenario with a CO_2 concentration of ~700 ppm by 2100, to simulate future climate. The climate scenario outputs were taken from the study of the National Climate Center, Chinese Meteorological Administration (Gao and others, 2010). The climate model was run for the entire region of China and surrounding areas, with a horizontal resolution of 25 km and 288 × 138 gridpoints. RegCM3 was described extensively by Pal and others (2007).

HBV hydrological model

To simulate river discharge, we used the HBV hydrological model developed by the Swedish Meteorological and Hydrological Institute (SMHI). The original version of the HBV model was used for runoff simulation and hydrological forecasts on Swedish lowlands (Bergström, 1976) and later extended for application in glaciated alpine catchments (Braun and Renner, 1992). A wide variety of model applications to catchments including the European Alps (Braun and others, 2000; Konz and Seibert, 2010), the Tien Shan (Hagg and others, 2006), the Himalaya (Akhtar and others, 2009) and other regions (Wang and others, 2006) have demonstrated the robust performance of the model and its capabilities for solving various hydrological problems. These included runoff modeling with respect to the effects of climate change on the water availability of alpine river basins (Hagg and others, 2007), the forecast of extreme runoff events (Akhtar and others, 2008) and the development of appropriate strategies for sustainable water management.

The HBV model is a semi-distributed, conceptual precipitation–runoff model using sub-basins as the primary hydrological unit. The model takes into account area–elevation distribution and basic land use categories (glaciers, forests, fields and lakes). Sub-basins are considered in geographically or climatologically heterogeneous basins (SMHI, 2006). The model has a clear structure and requires few parameters for its calculations, and these parameters have physical meanings. The model consists of subroutines for snow accumulation and melt, a soil-moisture accounting procedure, routines for runoff generation, and a simple routing procedure. It works on a daily time step and has a low data demand: only daily mean air temperature and precipitation, long-term mean monthly potential evaporation, and daily discharge are required for calibration. We calibrated the model parameters manually. To assess the agreement between modeled and measured discharge, we calculated the Nash–Sutcliffe efficiency (R^2) (Nash and Sutcliffe, 1970) and the relative error (RE):

$$R^2 = 1 - \frac{\sum_{i=1}^{i=N} [Q_s(i) - Q_o(i)]^2}{\sum_{i=1}^{i=N} \left[Q_o(i) - \overline{Q_o}\right]^2} \quad (1)$$

$$\mathrm{RE} = 100 \frac{\sum_{i=1}^{i=N} [Q_s(i) - Q_o(i)]}{\sum_{i=1}^{i=N} Q_o(i)} \quad (2)$$

where i is the time step, N is the total number of time steps, Q_s is simulated discharge, Q_o is observed discharge and $\overline{Q_o}$ is the mean of Q_o over the calibration/validation period. A perfect model would result in an r^2 value of 1 and an RE value close to zero.

RESULTS AND DISCUSSION

Modeling with the observed climate

Calibration and validation of the HBV model

The model was calibrated using daily discharge observations for the period 1997–2008 in the two study areas, and validation runs were performed for 1986–95. These two time periods not only included relatively dry and wet years, but also covered sufficient observational data to calibrate and verify the model. For the glacier No. 1 catchment, glacier mass balance and discharge data were also used in the calibration procedure to determine the appropriate parameters for the snow and glacier routine. Mass-balance measurements were unavailable for the other six glaciers except for glacier No. 1 in Zongkong catchment. Prior knowledge of the study areas, in combination with significant experience in parameter estimation gained in previous HBV studies, helped us to acquire suitable values for the main parameters. During the calibration period, the parameters *TT*, *DTTM*, *CFMAX* and *GMELT,* defined in Table 2, were found to be most sensitive, followed by the parameters *FC* and *PERC*. Additionally, these parameters were strongly interdependent. Table 2 lists the values of the sensitive parameters for the two sub-basins after calibration.

Figure 2 compares the simulated and observed discharge for the periods of calibration (1997–2008) and validation (1986–95) for the two basins. Daily discharges are only displayed from May to September for each year because >95% of the annual runoff at the stations occurs during this period; the rivers are mostly frozen for the rest of the year. The discharge in daily timescale in Figure 2 shows the close matches between simulated and observed values in the two catchments. Table 3 lists the R^2 and RE values for the daily calibration and validation: all the mean R^2 values are >0.7, and RE values are in the range of ±5%, indicating satisfactory model performance. The annual sums of the simulated and observed discharges also confirmed satisfactory model performance: the correlation coefficients were 0.85 for Ürümqi glacier No. 1 and 0.77 for Zongkong. The overall

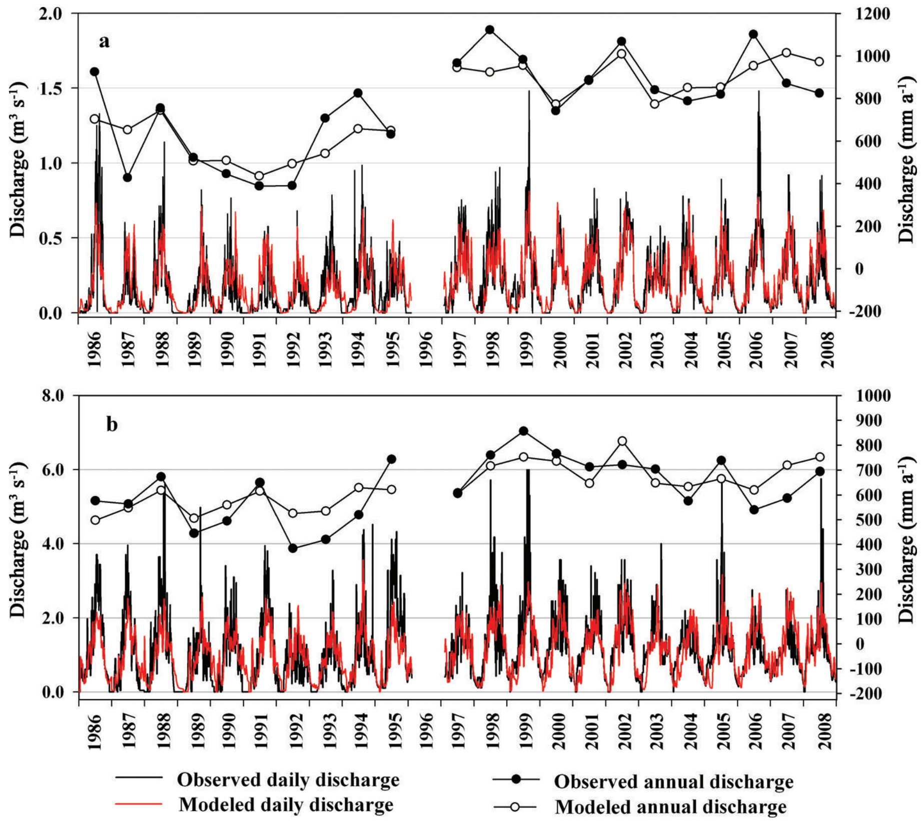

Fig. 2. Time series of modeled and observed discharges for (a) Ürümqi glacier No. 1 and (b) Zongkong monitoring stations. Daily discharges at the two stations are recorded from May to September of each year.

performance of the model was better for the calibration periods than for the validation periods at the two monitoring stations. Additionally, both calibration results were underestimated with respect to observations, and both validation simulations were overestimated with respect to observations at the two catchments. Specifically, in the glacier No. 1 catchment, the model slightly underestimated the total discharge in 1986, 1993, 1994 and 1998, and overestimated the total discharge in 1987, 2007 and 2008. In the Zongkong catchment, the model slightly overestimated the observed total runoff in 1992, 2007 and 2008, and slightly underestimated the total runoff in 1986 and 1999. This was

Table 2. Sensitive parameters and optimal values of HBV for the two study areas

Parameter	Description	Glacier No. 1	Zongkong	Unit
TT	Temperature limit for snow/rain	2.3	2	°C
DTTM	Value added to *TT* to give threshold temperature for snowmelt	–3.3	–3.8	°C
CFMAX	Snowmelt factor	2.7	3.4	mm °C^{-1} d^{-1}
GMELT	Glacier melt factor	4.5	5.1	mm °C^{-1} d^{-1}
FC	Maximum soil moisture storage	300	500	mm
PERC	Percolation from upper to lower response box	0.132	0.35	mm d^{-1}

Table 3. Efficiency criteria of modeling performance for the two study areas (R^2 is from Eqn (2), RE is from Eqn (3))

Catchment	Period	R^2_{mean}	R^2_{min}	R^2_{max}	RE %
Ürümqi glacier No. 1	Calibration (1997–2008)	0.81	0.65	0.91	–4 ± 1
	Validation (1986–95)	0.71	0.62	0.83	5 ± 3
Zongkong	Calibration (1997–2008)	0.77	0.74	0.87	–2 ± 1
	Validation (1986–95)	0.75	0.72	0.8	3 ± 2

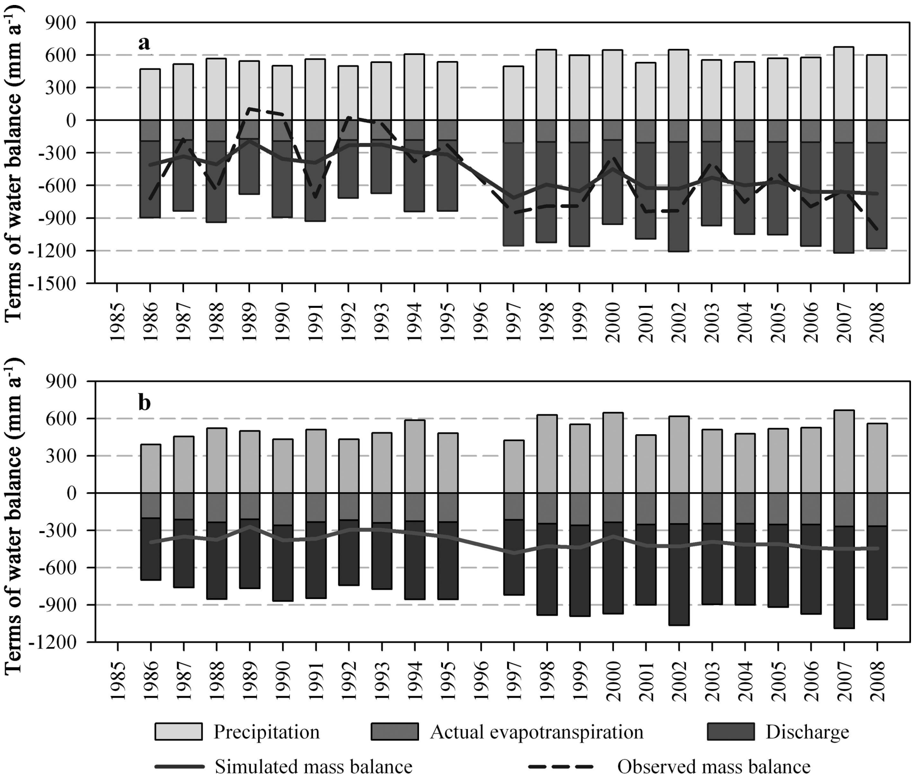

Fig. 3. Main terms of modeled water balance for (a) Ürümqi glacier No. 1 and (b) Zongkong catchments. Components with a positive sign are inputs into the system; components with a negative sign are outputs from the system.

probably caused by using constant values for the parameters for the whole simulation period. Compared with the observed discharges, the relative errors for simulated discharges were within ±5%. According to the rate-modeling performance of Moriasi and others (2007), the accuracy was acceptable. Furthermore, the annual changes in the simulated mass storage of Ürümqi glacier No. 1 also coincided well with the measured values (see Fig. 3a). The simulations and observations had a correlation coefficient of 0.86, significant at the 1% level, which demonstrated that the HBV model was capable of simulating the discharge regime adequately and was suitable for this study.

Annual water balance

Figure 3 shows the temporal variations in the individual terms of the water balance of the Ürümqi river source area from 1986 to 2008, excluding 1996. The two catchments had several common characteristics in terms of the simulated annual water balance volume. Clearly, discharge was by far the largest component of the water balance, followed by basin precipitation. Evapotranspiration in the periods 1986–95 and 1996–2008 generally remained unchanged. The simulated discharge and mass balance of the glaciers during the calibration period were larger than those in the validation period, consistent with the observed records in the two catchments. For the Ürümqi glacier No. 1 catchment, the discharge was in excellent agreement with the simulated mass balance. In other words, discharge was generally large in years with high mass losses. Given the relatively steady precipitation, these results suggest that enhanced glacier mass losses contributed significantly to the change in discharge. However, for the Zongkong catchment, the change in discharge consistently matched the precipitation, which was possibly related to the small area of glacier coverage in this catchment. Table 4 lists each component of the water balance during the calibration and validation periods in the two catchments. A notable result was that the annual changes in overall storage of the two catchments were negative, and the rates of these changes were faster from 1997 to 2008 than from 1986 to 1995. The storage term summarizes the changes in water storage in snowpack, soil, groundwater and glacier. Snowpack, soil and especially groundwater exhibited small changes ($\Delta UZ + \Delta LZ$): they played a minor role and their volumes are considered to be almost negligible in the two catchments. However, changes in glacier storage varied greatly over the simulation period, and values were negative in all the years of the study period. This finding suggests continual mass losses, which (with the exceptions of 1989, 1990 and 1992) is also supported by the findings of Jing and others (2006), the World Glacier Monitoring Service (WGMS, 2009) and Li and others (2011), who measured the rapid retreat and mass losses of glacier No. 1 over the past two decades. This result demonstrates that glacier melt and runoff makes a major contribution to the water balance of the catchment. Figure 3 and Table 4 further show that the fluctuations in computed water balance elements during the calibration period were much larger than those during the validation period, which may be related to the intensified water cycle expected from the climate warming of recent years (Wang and others, 2014).

Modeling results with future climate

After the successful calibration and validation of the HBV model using the observed climate variables, the statistically downscaled temperature and precipitation of RegCM3 were used to drive the model to estimate the variation in future water resources.

Table 4. Water balance terms (mm a^{-1}) for the study area catchments as calculated using the HBV model (*P*: basin precipitation; *E*: basin evapotranspiration; *Q*: discharge; ΔSnow: change in snow storage; ΔSM: change in soil moisture storage; Δ*UZ*: water content change of upper box; Δ*LZ*: water content change of lower box; ΔGlacier: change in glacier storage; Annual change: annual change in overall storage)

Catchment	Period	*P*	*E*	*Q*	Storage change					Annual change
					ΔSnow	ΔSM	Δ*UZ*	Δ*LZ*	ΔGlacier	
Glacier No. 1	1986–95	534	186	637	12	15	2	–4	–314	–28.9
	1997–2008	589	202	909	–5	36	5	5	–563	–43.5
Zongkong	1986–95	503	223	575	9	6	2	–2	–310	–29.5
	1997–2008	567	247	710	–1	15	2	–3	–403	–32.5

Table 5. Statistical parameters for relationships between the observed and projected data. *T*: monthly mean air temperature (°C a^{-1}); *P*: monthly precipitation (mm a^{-1}); *r*: correlation coefficient; r^2: degree of determination, i.e. the variance or square of the correlation coefficient

Variable	a_1	a_2	a_3	a_4	b	r	r^2
T	2.744	–2.923	0	0.897	–0.994	0.963	0.927
P	0	0.398	0	0	1.384	0.822	0.676

Changes in temperature and precipitation from 2041 to 2060

Wu and others (2011) systematically studied the annual, winter and summer spatial distributions of temperature and precipitation based on the RegCM3 model, and confirmed that the projected temperature and precipitation during 1981–2000 from RegCM3 were in close agreement with the observed data in the Tien Shan. Nevertheless, the meteorological outputs from the climate model were not applied directly to our hydrological applications, because they were unable to represent local subgrid-scale features and dynamics, despite the fact that RegCM3 has a high-resolution spatial scale (Giorgi and Francisco, 2000). Therefore, we applied a simple statistical downscaling method, a nonlinear regression, which involved establishing a nonlinear relationship between a large-scale average surface variable and the local-scale variable (Chen and others, 2011). We built a relationship between the observed data at the Daxigou meteorological station and the projected climate variables from RegCM3 at four neighboring gridpoints for 1961–2000. The future daily temperature and precipitation time series in the A1B emission scenario were calculated using (Wilby and others, 1998)

$$y = a_1x_1 + a_2x_2 + a_3x_3 + a_4x_4 + b \quad (3)$$

where y is a future time series of temperature or precipitation, x is a projected temperature or precipitation time series (using RegCM3) and a_1, a_2, a_3, a_4 and b are parameters whose values are listed in Table 5.

The future projections of temperature and precipitation strongly depend on the surrounding orographic conditions with different spatial correlations. As a whole, correlations for precipitation are lower than those for temperature (Table 5). This is likely because the spatial variability of precipitation in the mountains is high. The histograms of the residual indicate that the data follow an approximately normal distribution without significant outliers (Fig. 4) and that the validity of the above downscaling method is acceptable for the present study. According to the above statistical relationship, the temperature and precipitation time series (1961–2000) derived from downscaling from RegCM3 agree closely with the observational data at Daxigou meteorological station. Correlation coefficients are 0.963 and 0.822, respectively, demonstrating that the statistical relationships perform well.

Figure 5 shows the potential variation of temperature and precipitation projected by RegCM3 based on the SRES A1B scenario for 2041–60 relative to 2000–08. A clear temperature increase was observed in all months. Temperature increases reached a maximum of 2.0°C in August and a minimum of 1.0°C in December. The annual mean

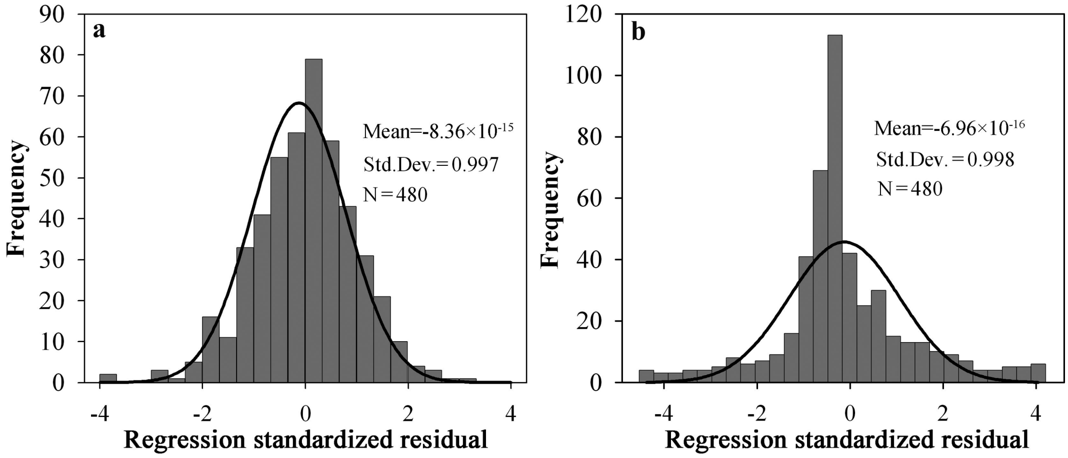

Fig. 4. Histogram of the residual of (a) temperature and (b) precipitation.

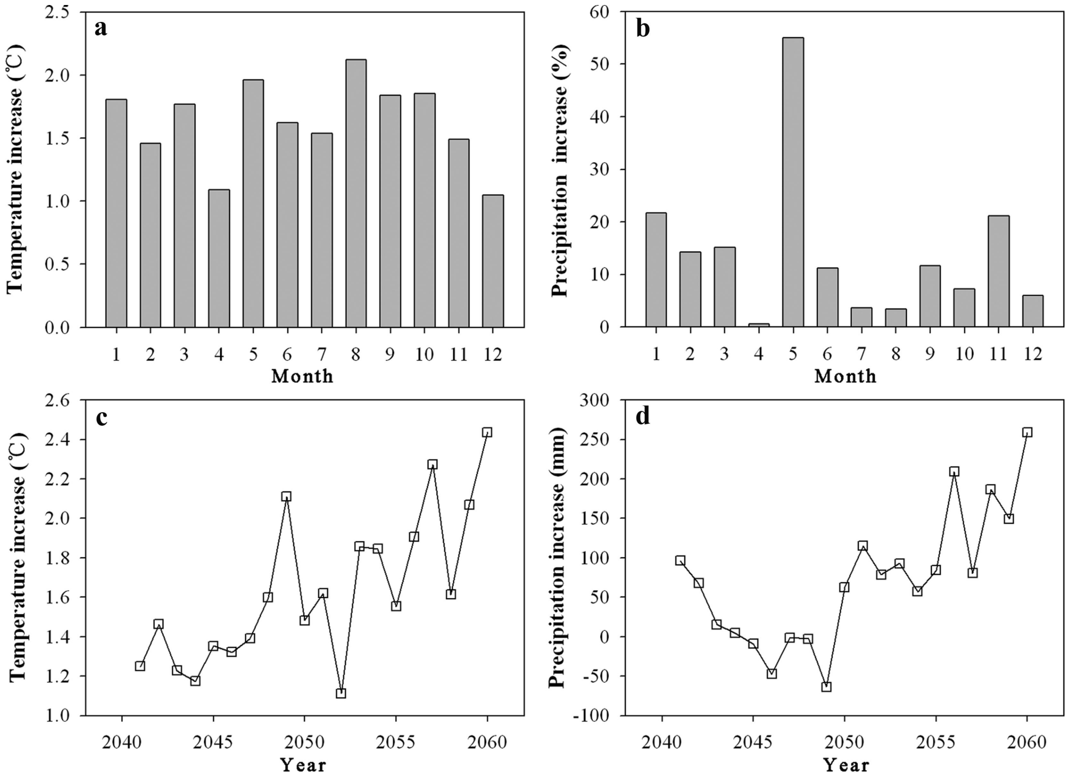

Fig. 5. Monthly (a, b) and yearly (c, d) variations in precipitation derived from downscaling from RegCM3 under SRES A1B scenario for 2041–60 relative to 2000–08.

temperature rose to 1.7°C for the period 2041–60. In general, precipitation was projected to increase, although with a downward trend in the first few years. Based on monthly changes, the mean annual cycle of precipitation exhibited more variability than the mean annual cycle of temperature. One significant finding was that almost no change in precipitation appeared in April, but precipitation reached a maximum increase of 55% in May under the forced scenario. Annual precipitation was predicted to increase by 14.2% by the mid-21st century. The overall increases in temperature and precipitation were consistent with the findings of Hagg and others (2007) and Akhtar and others (2008), who projected that temperature and precipitation in central Asia and the Hindu Kush–Karakoram–Himalaya region will increase.

Future annual discharge cycle

Figure 6 shows the average monthly modeled results for the baseline period (2000–08) and future climate scenario (2041–60, SRES A1B scenario) with three stages of glacier coverage (i.e. compared to the glacier coverage in 2008): unchanged glacier size (100% glacierized), recession of half the glacier area (50% glacierized) and complete disappearance of glaciers (0% glacierized). Table 6 presents the mean changes and their standard deviations ($\pm 1\sigma$) in the estimated future discharge for the three glaciation stages relative to the discharge during 2000–08 in the two catchments. The three stages of glacier coverage are described and discussed below.

1. *100% glacierized.* With no change in the average glaciated area during 2041–60, compared with baseline conditions (2008), river discharge increases throughout the melt season in the projected climate for the two basins compared with the mean modeled discharge for 2000–08 (Fig. 6). This is an expected response to increasing temperatures and precipitation in a warming climate, and primarily reflects that snowmelting starts half a month earlier than in the period 2000–08, with discharge peaking in the summer months. The 100% glacierized scenario predicted a significant increase in discharge in the Ürümqi glacier No. 1 catchment (66% on average,

Table 6. Mean changes in future discharge (2041–60) under A1B emission scenarios relative to the discharge (2000–08) for three glaciated areas in two catchments. To account for the uncertainty in projected discharge, the standard deviations of the changes ($\pm 1\sigma$) are given

Catchment	Month	Measured discharge in 2000–08	Change in future discharge		
			100% glacierized	50% glacierized	0% glacierized
		mm	%	%	%
Glacier No. 1	May	11	106 ± 88	65 ± 51	61 ± 43
	Jun	135	129 ± 74	27 ± 26	–17 ± 22
	Jul	334	38 ± 10	–24 ± 5	–68 ± 5
	Aug	301	53 ± 16	–189 ± 11	–72 ± 5
	Sep	55	162 ± 49	26 ± 14	–51 ± 23
	Annual	852	66 ± 35	–8 ± 5	–58 ± 20
Zongkong	May	28	183 ± 117	140 ± 102	135 ± 99
	Jun	162	28 ± 4	–14 ± 3	–42 ± 7
	Jul	230	17 ± 2	–22 ± 2	–54 ± 3
	Aug	205	26 ± 5	–19 ± 4	–56 ± 4
	Sep	65	64 ± 14	2 ± 1	–42 ± 28
	Annual	719	33 ± 20	–9 ± 6	–40 ± 13

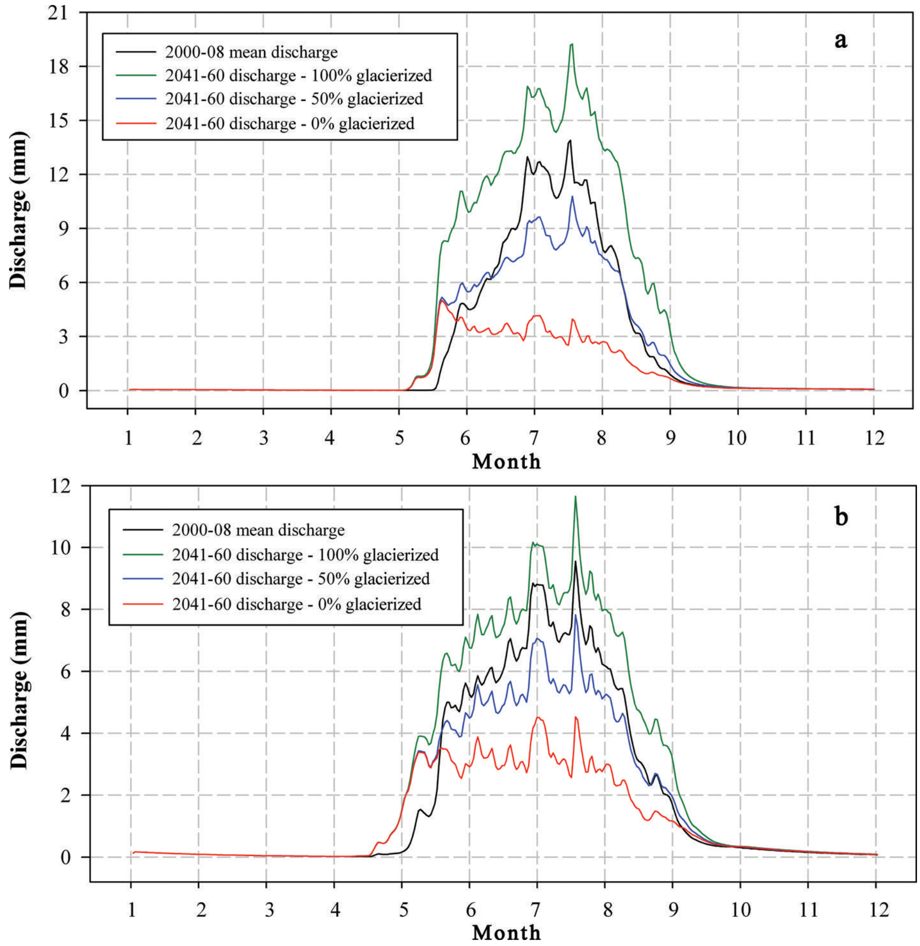

Fig. 6. Annual discharge cycle of (a) Ürümqi glacier No. 1 and (b) Zongkong catchments simulated by HBV for current climate (2000–08) and future climate (2041–60) for three stages of glacierization.

$\sigma = 35\%$) and a relatively small increase in the Zongkong catchment (33% on average, $\sigma = 20\%$) (Table 6). These findings indicate that a heavily glaciated catchment is likely to produce more variation in discharge compared with a less glaciated catchment. Additionally, compared with the discharge in 2000–08, the magnitude of the future rise in discharge is significantly higher in May, June and September, when the simulated results have larger standard deviations. This is partly because the two basins have a low volume of discharge during the three months, and a small absolute increase can lead to a larger perceived change in discharge relative to July and August, when the largest volumes are observed and the range of uncertainty is smaller. However, this case is only a hypothetical result of our study, and might not actually occur in the future. Thus, it can only be presented as a possible trend because the glacier area will likely diminish drastically after such intense climate change.

2. *50% glacierized.* If the glacier area is reduced by half (i.e. a reduction from 50% to 25% in the glacier No. 1 catchment and from 18% to 9% in the Zongkong catchment), snowmelt will still begin half a month earlier and discharge will increase in May and September (Fig. 6), due to more frequent rainfall and a prolonged period of snow and glacier melt caused by regional climate warming. The discharge in July and August decreases significantly, but the peak discharge for the two stations remains concentrated in these two months (Fig. 6). On an annual timescale, this scenario predicted no clear changes, with a slight decrease (8% on average, $\sigma = 5\%$) in the glacier No. 1 catchment and a small decrease (9% on average, $\sigma = 6\%$) in the Zongkong catchment (Table 6), probably due to the decrease in glacier area being nearly balanced out by the increased melt rates.

3. *0% glacierized.* After complete disappearance of the glaciers, snowmelt still started half a month earlier and discharge increased in May. A pronounced decrease in discharge is predicted from June to September (Fig. 6). In the Ürümqi glacier No. 1 catchment, a $58 \pm 20\%$ decrease in annual discharge is predicted, with the greatest decline reaching $72 \pm 5\%$ in August (Table 6). The most striking feature of these results is the clear seasonal shift in peak discharge, from midsummer to late spring/early summer by mid-century. For the Zongkong catchment, a drastic decrease in discharge is also predicted ($40 \pm 13\%$). Again, the greatest decline occurs in July and August, when discharge is predicted to be reduced by $54 \pm 3\%$ and $56 \pm 4\%$, respectively (Table 6). This finding illustrates the important contribution of glaciers to total discharge in the two basins. No forest or major lake is situated in the two sub-basins, and glaciers and bare land (unforested area) were the only two land use types considered in the hydrological model framework. Therefore, the effect of complete melting of the glaciers on the hydrological cycle will depend on the degree of glaciation in the river basins and the response

of the river basins to climate change. The significant decrease in discharge may aggravate the existing water shortage crisis in this region, especially in July and August, when demand for water for agricultural production peaks. The temperature increase will also lead to increased snowmelt runoff, which may occur more frequently, and earlier spring runoff, and will ultimately cause more changes in the amount and timing of runoff and the reallocation of intra-annual water resources in the catchment.

Model limitations

The glacier hydrological processes in the Ürümqi river source area were successfully simulated using an HBV model, and the possible effects of future climate on the hydrological cycle on the watershed were quantified and evaluated. The findings provide valuable information for future water resource management. However, this modeling study had several limitations: While the model projected future discharge, its parameters of glacial ablation were based on data observed from 1986 to 2008, and did not take into account possible changes in ablation rates as the glacier retreats or is progressively confined to favorable topographic areas by mid-century. The critical parameters listed in Table 2, *TT*, *DTTM*, *CFMAX* and *GMELT*, will certainly change with climate change. Such parameters can dramatically influence glacier response to climate forcing and may significantly alter the simulated melt and projected discharge. When considering the effects of landscape type, we assumed that areas of glacier retreat are covered by bare land. Although this is a reasonable assumption (and currently only glacier and bare land are observed above 3500 m a.s.l. at the Ürümqi river source area), the landscape may possibly evolve along with significant climate change and the extension of human activities toward the high mountains. Additionally, the expected pattern of glacier retreat is from its terminus to the top, suggesting a more complex situation than originally assumed. According to the observations of Li (2005), a supraglacial lake with an area of 30 m^2 appeared at the top of the east branch of glacier No. 1, and a region without snow was found at 4425 m a.s.l., suggesting that the glacier had begun to melt in the accumulation area. Moreover, the three scenarios of glacier recession in our study are hypothetical because the HBV model is not capable of describing deglaciation in an iterative way, and the study used one regional climate model under only one greenhouse gas emission scenario (SRES-A1B).

CONCLUSIONS

We linked the HBV hydrological model and RegCM3 regional climate models to project the effects of future climate change, under SRES A1B conditions, on river discharge in the Ürümqi river source region under three scenarios of glacier coverage. The climate input data for the HBV model were taken from observed meteorological data, and the downscaled data from the output of the RegCM3. Using observed data for the period 1985–2008 (excluding 1996), the calibration and validation results demonstrated that the HBV model adequately reproduced discharge, except for peak values, which were slightly underestimated for certain years. Variations in temperature and precipitation in the study area were also captured satisfactorily by the RegCM3, with a projected general increase in temperature and precipitation by mid-century (2041–60). Under the altered climate conditions, snowmelt will begin half a month earlier, and discharge in May will increase for all glacier coverage scenarios in both catchments. These findings suggest that the temperature increase will cause more frequent rainfall and increased snowmelt runoff, which may consequently increase the volume of river water during spring. The 100% glacierized scenario predicted a pronounced increase in river discharge in the two basins. Discharge is predicted to increase by $33 \pm 20\%$ in the Zongkong catchment and by $66 \pm 35\%$ in the glacier No. 1 catchment by mid-century. The 50% glacierized scenario predicted a slight decrease in discharge. However, the 0% glacierized scenario predicted a substantial decrease in discharge in the glacier No. 1 catchment ($58 \pm 20\%$) and the Zongkong catchment ($40 \pm 13\%$), especially in July and August when demand for water for agricultural production currently peaks. This scenario may therefore aggravate the water shortage crisis in the region. Complete disappearance of the glacier will result in a significant temporal shift in the hydrological patterns of water resources from midsummer to late spring/early summer by mid-century in the glacier No. 1 catchment. Based on our results, we conclude that climate warming and the resulting glacier shrinkage will cause significant changes in the amount and timing of runoff and will ultimately result in the reallocation of intra-annual water resource utilization in the catchment.

ACKNOWLEDGEMENTS

This research was supported by the National Science and Technology Support Program of China (No. 2012BAC19B07), the National Natural Science Foundation of China (No. 41261016) and the Project of Scientific Ability Promoting Young Teachers of Northwest Normal University (No. NWNU-LKQN-12-20). We thank Gao Xuejie of the National Climate Center, Chinese Meteorological Administration, for providing the RegCM3 projected data. We also thank the anonymous reviewers and the Chief Editor, T.H. Jacka, for valuable comments.

REFERENCES

Akhtar M, Ahmad N and Booij MJ (2008) The impact of climate change on the water resources of Hindukush–Karakorum–Himalaya region under different glacier coverage scenarios. *J. Hydrol.*, **355**(1–4), 148–163 (doi: 10.1016/j.jhydrol.2008.03.015)

Akhtar M, Ahmad N and Booij MJ (2009) Use of regional climate model simulations as input for hydrological models for the Hindukush–Karakorum–Himalaya region. *Hydrol. Earth Syst. Sci.*, **13**(7), 1075–1089 (doi: 10.5194/hess-13-1075-2009)

Bergström S (1976) *Development and application of a conceptual runoff model for Scandinavian catchments.* (Bulletin Series A 52) Lund Institute of Technology, University of Lund, Lund

Braun LN and Renner CB (1992) Application of a conceptual runoff model in different physiographic regions of Switzerland. *Hydrol. Sci. J.*, **37**(3), 217–231 (doi: 10.1080/02626669209492583)

Braun LN, Weber M and Schulz M (2000) Consequences of climate change for runoff from Alpine regions. *Ann. Glaciol.,* **31**, 19–25 (doi: 10.3189/172756400781820165)

Chen J, Brissette FP and Leconte R (2011) Uncertainty of downscaling method in quantifying the impact of climate change on hydrology. *J. Hydrol.*, **401**(3–4), 190–202 (doi: 10.1016/j.jhydrol.2011.02.020)

Gao X, Shi Y and Giorgi F (2010) A high resolution simulation of climate change over China. *Sci. China: Earth Sci.*, **54**(3), 462–472 (doi: 10.1007/s11430-010-4035-7)

Giorgi F and Francisco R (2000) Evaluating uncertainties in the prediction of regional climate change. *Geophys. Res. Lett.*, **27**(9), 1295–1298 (doi: 10.1029/1999GL011016)

Giorgi F, Marinucci MR and Bates GT (1993a) Development of a second generation regional climate model (RegCM2). Part I. Boundary layer and radiative transfer processes. *Mon. Weather Rev.*, **121**(10), 2794–2813 (doi: 10.1175/1520-0493(1993)121<2794:DOASGR>2.0.CO;2)

Giorgi F, Marinucci MR, Bates GT and DeCanio G (1993b) Development of a second generation regional climate model (RegCM2). Part II. Convective processes and assimilation of lateral boundary conditions. *Mon. Weather Rev.*, **121**(10), 2814–2832 (doi: 10.1175/1520-0493(1993)121<2814:DOASGR>2.0.CO;2)

Hagg W, Braun LN, Weber M and Becht M (2006) Runoff modelling in glacierized Central Asian catchments for present-day and future climate. *Nord. Hydrol.*, **37**(2), 93–105

Hagg W, Braun LN, Kuhn M and Nesgaard TI (2007) Modelling of hydrological response to climate change in glacierized Central Asian catchments. *J. Hydrol.*, **332**(1–2), 40–53 (doi: 10.1016/j.jhydrol.2006.06.021)

Han T, Gao M, Ye B and Jiao K (2010) Characteristic of runoff process of the glacier and permafrost in the headwaters of the Urumqi River. *J. Glaciol. Geocryol.*, **32**(3), 573–579 [in Chinese]

Immerzeel WW, Van Beeke LPH and Bierkens MFP (2010) Climate change will affect the Asian water towers. *Science*, **328**(5984), 1382–1385 (doi: 10.1126/science.1183188)

Jing Z, Jiao K, Yao T, Wang N and Li Z (2006) Mass balance and recession of Ürümqi glacier No. 1, Tien Shan, China, over the last 45 years. *Ann. Glaciol.,* **43**, 214–215 (doi: 10.3189/172756406781811899)

Konz M and Seibert J (2010) On the value of glacier mass balances for hydrological model calibration. *J. Hydrol.*, **385**(1–4), 238–246 (doi: 10.1016/j.jhydrol.2010.02.025)

Li Z (2005) A glacier melt water pool was discovered at summit of the east branch of the Glacier No. 1 at Ürümqi River head, Tianshan Mts., Xinjiang. *J. Glaciol. Geocryol.*, **27**(1), 150–152 [in Chinese]

Li Z, Li K and Wang L (2010a) Study on recent glacier changes and their impact on water resources in Xinjiang, Northwestern China. *Quat. Sci.*, **30**(1), 96–106 [in Chinese] (doi: 10.3969/j.issn.1001-7410.2010.01.09)

Li Z, Wang W, Zhang M, Wang F and Li H (2010b) Observed changes in streamflow at the headwaters of the Urumqi River, eastern Tianshan, central Asia. *Hydrol. Process.*, **21**(2), 217–224 (doi: 10.1002/hyp.7431)

Li Z, Li H and Chen Y (2011) Mechanisms and simulation of accelerated shrinkage of continental glaciers: a case study of Urumqi Glacier No. 1 in eastern Tianshan, Central Asia. *J. Earth Sci.*, **22**(4), 423–430 (doi: 10.1007/s12583-011-0194-5)

Liu C, Kang E, Liu S, Chen J and Liu Z (1999) Study on glacier variation and its runoff responses in the arid region on Northwest China. *Sci. China D,* **42**, Suppl. 1, 64–71 (doi: 10.1007/BF02878854)

Liu J and 15 others (2014) Spatiotemporal characteristics, patterns, and causes of land-use changes in China since the late 1980s. *J. Geogr. Sci.*, **24**(2), 195–210 (doi: 10.1007/s11442-014-1082-6)

Liu S, Sun W, Shen Y and Li G (2003) Glacier changes since the Little Ice Age maximum in the western Qilian Shan, northwest China, and consequences of glacier runoff for water supply. *J. Glaciol.*, **49**(164), 117–124 (doi: 10.3189/172756503781830926)

Liu S and 7 others (2006) Glacier retreat as a result of climate warming and increased precipitation in the Tarim river basin, northwest China. *Ann. Glaciol.,* **43**, 91–96 (doi: 10.3189/172756406781812168)

Mark BG and Seltzer GO (2003) Tropical glacier meltwater contribution to stream discharge: a case study in the Cordillera Blanca, Peru. *J. Glaciol.*, **49**(165), 271–282 (doi: 10.3189/172756503781830746)

Moriasi DN, Arnold JG, Van Liew MW, Bingner RL, Harmel RD and Veith VL (2007) Model evaluation guidelines for systematic quantification of accuracy in watershed simulation. *Trans. Am. Soc. Agric. Biol. Eng.*, **50**(3), 885–900

Nash JE and Sutcliffe JV (1970) River flow forecasting through conceptual models. Part 1. A discussion of principles. *J. Hydrol.*, **10**(3), 282–290 (doi: 10.1016/0022-1694(70)90255-6)

Pal JS and 19 others (2007) Regional climate modeling for the developing world: the ICTP RegCM3 and RegCNET. *Bull. Am. Meteorol. Soc.*, **88**(9), 1395–1409 (doi: 10.1175/BAMS-88-9-1395)

Shangguan D and 8 others (2007) Glacier changes in the west Kunlun Shan from 1970 to 2001 derived from Landsat TM/ETM+ and Chinese glacier inventory data. *Ann. Glaciol.*, **46**, 204–208 (doi: 10.3189/172756407782871693)

Shi Y and Kang E (1992) *Formation and estimation of water resources in mountainous regions of the Ürümqi River*. Science Press, Beijing [in Chinese]

Solomon S and 7 others eds (2007) *Climate change 2007: the physical science basis. Contribution of Working Group I to the Fourth Assessment Report of the Intergovernmental Panel on Climate Change*. Cambridge University Press, Cambridge

Stahl K, Moore RD, Shea JM, Hutchinson D and Cannon AJ (2008) Coupled modelling of glacier and streamflow response to future climate scenarios. *Water Resour. Res.*, **44**(W24), W02422 (doi: 10.1029/2007WR005956)

Sun M, Li Z, Yao X and Ji S (2013) Rapid shrinkage and hydrological response of a typical continental glacier in the arid region of northwest China – taking Urumqi Glacier No.1 as an example. *Ecohydrology*, **6**(6), 909–916 (doi: 10.1002/eco.1272)

Swedish Meteorological and Hydrological Institute (SMHI) (2006) *Integrated hydrological modelling system (IHMS) manual, version 5.10*. Swedish Meteorological and Hydrological Institute, Norrköping

Viviroli D, Dürr HH, Messerli B, Meybeck M and Weingartner R (2007) Mountains of the world, water towers for humanity: typology, mapping, and global significance. *Water Resour. Res.*, **47**(7), W07447 (doi: 10.1029/2006WR005653)

Wang S, McGrath R, Semmler T, Sweeney C and Nolan P (2006) The impact of the climate change on discharge of Suir River Catchment (Ireland) under different climate scenarios. *Natur. Hazards Earth Syst. Sci. (NHESS)*, **6**(3), 387–395 (doi: 10.5194/nhess-6-387-2006)

Wang S and 6 others (2014) Comparison of surface air temperature derived from NCEP/DOE R2, ERA-Interim, and observations in the arid northwestern China: a consideration of altitude errors. *Theor. Appl. Climatol.* (doi: 10.1007/s00704-014-1107-1)

Wilby R and 6 others (1998) Statistical downscaling of general circulation model output: a comparison of methods. *Water Resour. Res.*, **34**(11), 2995–3008 (doi: 10.1029/98WR02577)

World Glacier Monitoring Service (WGMS) (2009) *Glacier Mass Balance Bulletin No. 10 (2006–2007)*, ed. Haeberli W, Gärtner-Roer I, Hoelzle M, Paul F and Zemp M. ICSU(WDS)/IUGG (IACS)/UNEP/UNESCO/WMO, World Glacier Monitoring Service, Zürich, 36–39

Wu J, Gao X, Shi Y and Giorgi F (2011) Climate change over Xinjiang Region in the 21st century simulated by a high resolution regional climate model. *J. Glaciol. Geocryol.*, **33**(3), 479–487 [in Chinese]

Ye B and 6 others (2005) The Ürümqi River source Glacier No. 1, Tianshan, China: changes over the past 45 years. *Geophys. Res. Lett.*, **32**(21), L21504 (doi: 10.1029/2005GL024178)

MS received 20 February 2014 and accepted in revised form 8 November 2014